

# **Fracture Permeability in the Barnett Shale: Effects of Roughness, Fracture Offset, Proppant, and Effective Stress\***

**Sarah M. Kassis<sup>1</sup>**

Search and Discovery Article #80188 (2011)

Posted September 26, 2011

\*Adapted from poster presentation at AAPG Annual Convention and Exhibition, Houston, Texas, USA, April 10-13, 2011

<sup>1</sup>University of Oklahoma; currently Gulf Coast Business Unit, ConocoPhillips, Houston, TX ([sarah.m.kassis@conocophillips.com](mailto:sarah.m.kassis@conocophillips.com))

## **Abstract**

Domestic gas shale production is made economic through new completion practices which include horizontal wells and multiple hydraulic fractures. The performance of these fractures is improved through the injection of proppant. Success has largely been based on empiricism through field experiments. The attempt here to remove some uncertainty in this empiricism through a series of laboratory controlled experiments. We have measured the permeability of fractured rock as a function of effective stress, proppant, proppant distribution, and fracture offset. Our findings indicate that fracture offset is as effective as propping a fracture; both increase initial permeabilities more than 1000 fold over initial fracture values. However, the pressure dependence of the propped fracture is stronger; i.e., the permeability is reduced more per increment of pressure than the offset fractures. Neither obeys the simple cubic pressure dependence law proposed by Walsh. A simple monolayer of proppant is as effective as a fairway distribution of proppant in enhancing permeability. Initial fracture permeability is dependent on surface roughness, quantified as root mean square asperity heights. Pressure dependence of permeability of these fractured surfaces does obey the Walsh permeability models. SEM observations of surfaces and proppant suggest a new approach to proppant design.

## **Selected Bibliography**

Bernabe, Y., 1986, The effective pressure law for permeability in Chelmsford Granite and Barre Granite: International Journal of Rock Mechanics and Mining Sciences, v. 23, no. 3, p. 267-275.

Brown, S.E., 1987, Fluid flow through rock joints: The effect of surface roughness: Journal of Geophysical Research, v. 92, no. 2, p. 1337-1347.

Cook, N.G.W., 1992, Natural joints in rock-mechanical, hydraulic and seismic behavior and properties under normal stress (abstract): International Journal of Rock Mechanics and Mining Sciences and Geomechanics Abstracts, v. 29, p. 198-223.

Coulter, Gerald, R., Edward G. Benton, and Cliff Thompson, 2004, Water fracs and sand quantity: A Barnett Shale example: SPE 90891 (SPE Annual Technical Conference, Houston, TX, 26-29 September, 2004).

Gangi, A.F., 1978, Variation of whole and fractured porous rock permeability with confining pressure: International Journal of Rock Mechanics and Mining Sciences and Geomechanics Abstracts, v. 15, no. 5, p. 249-257.

Kranz, R.L., A.D. Frankel, T. Engelder, and C.H. Scholz, 1979, The permeability of whole and jointed Barre Granite: International Journal of Rock Mechanics and Mining Sciences, v. 16, p. 225-234.

Martineau, D.F., 2007, History of the Newark East Field and the Barnett Shale as a gas reservoir: AAPG Bulletin, v. 91, no. 4, p. 399-403.

Renshaw, C.E., 1995, On the relationship between mechanical and hydraulic apertures in rough-walled fractures: Journal of Geophysical Research, v. 100, no. 12, p. 24629-24636.

Schlumberger, 2007, Hydraulic fractures (<http://www.glossary.oilfield.slb.com/>) (accessed September 10, 2011)

Wash, J.B., 1981, Effect of pore pressure and confining pressure on fracture permeability: International Journal of Rock Mechanics and Mining Sciences, v. 18, p. 429-435.

# Fracture Permeability in the Barnett Shale: Effects of Roughness, Fracture Offset, Proppant, and Effective Stress

Sarah Kassis

University of Oklahoma  
Mewbourne School of Petroleum and  
Geological Engineering  
March 29, 2008

# Project Goal: Fracture Permeability

Influences:

- Roughness of fracture surfaces
- Fracture face offset
- Proppant
- Effective pressure

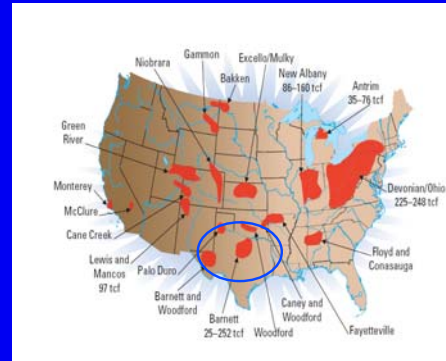


**Presenter's notes:** Goal: Study the effects of sample roughness, fracture-face offset, proppant, and effective pressure on permeability of gas shale samples.

# Gas Shales: Hold 1000 Tcf

## Characteristics:

- Impermeable: fluid does not flow through shale
  - Permeability must be created
- Production is driven by
  - Technology
  - Gas Price
- New resources: Barnett Shale



Schlumberger 2005

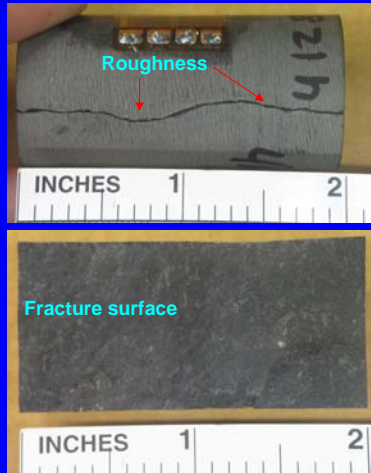
**Presenter's notes:** Gas shales are very tight formations which lack permeability, or the ability of hydrocarbons to flow through a formation. Permeability must be created in order to retrieve hydrocarbons through hydraulic fracturing.

Mitchell Energy drilled the first producing Barnett Shale well in 1981. Barnett is located in North-central Texas (Denton and Wise counties).

Production from shale plays is technology-driven, meaning everything we can do to increase permeability is important to maximizing return. Barnett Shale is a new play, and findings can be applied to other shales around the world, such as the Ootla shale play in Canada.

Assuming the United States consumes approximately 21 Tcf of gas every year, the gas in United States shale plays represents 48 years of U.S. gas consumption. Gas shale production became viable about twenty years ago with increase in gas price, which allowed technological improvement. In today's sensitive gas price environment, optimization is key to economic production.

# Experiments



- Four fractured shale samples
  - 8364 ft
  - 7828.7 ft
  - 7821 ft
  - 7766 ft
- Measure permeability
  - Starting surfaces
  - Offset surfaces
  - Proppant emplacement on surfaces
  - Under effective pressure

**Presenter's notes:** Four horizontal, cylindrical, uniaxial Barnett Shale samples were failed mechanically to produce fractures. Permeability was measured on: 1) the starting or virgin surfaces, which reflect the inherent roughness character of the samples, 2) surfaces with varying degrees of fracture face offset, 3) surfaces with 2 types of proppant in 2 configurations, and 4) all samples under an effective pressure range of 800-6000 psi.

# Instrumentation

- Samples imaged with SEM
  - Surface characteristics
  - Change in characteristics
- Permeability determined with commercial permeameter-porosimeter
  - 800 psi to 6000 psi



Scanning Electron Microscope

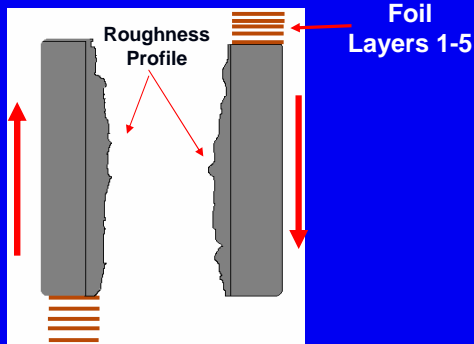


AP-608 permeameter-porosimeter

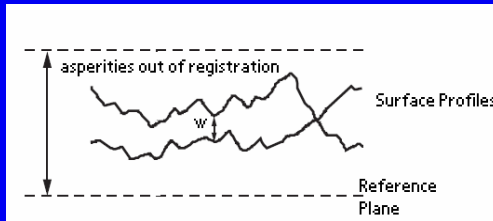
**Presenter's notes:** Samples were imaged with a scanning electron microscope (SEM) to monitor changes in surface characteristics and effects of roughness and proppant during the course of the experiments.

Permeability measurements were obtained with a commercial permeameter-porosimeter over an effective pressure range of 800-6000 psi.

# Fracture Offset



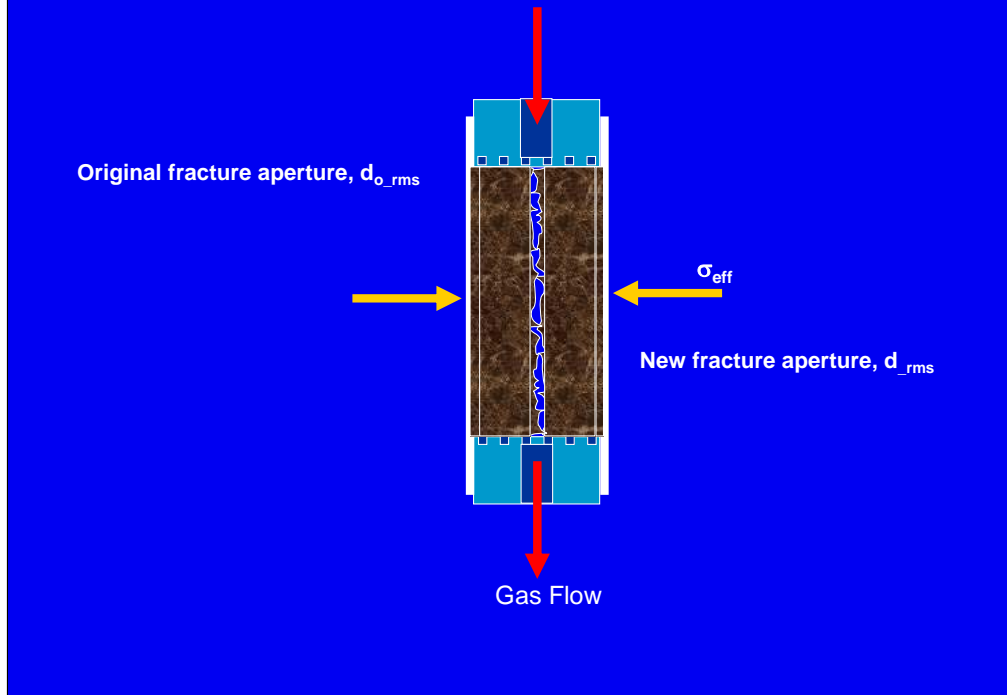
- Fracture faces misaligned
  - two mill .002" copper foil shims opposite ends of opposing half cylinders
  - 0.004" to 0.02" offset
- Causes asperities to move out of registration, aperture increase



**Presenter's notes:** After initial permeability measurements were taken, Fracture Face Offset experiments were performed on the four samples. The two faces of the fracture were misaligned using two mill (.002 inch) copper foil shims on opposite ends of the two fracture faces. The experiments were performed incrementally, increasing from 1 to 5 layers of copper foil, representing an offset of .004 inches up to .02 inches of offset. The effect of the copper shims is that the asperities, or relative highs on the surface of the fracture face, move out of registration, effectively propping the fracture open, and increasing the fracture aperture.



# Change in Fracture perm with increasing Effective Stress



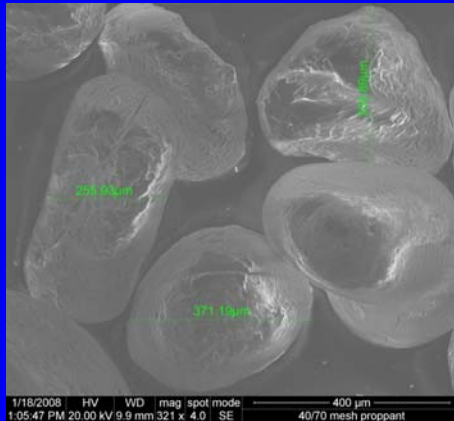
**Presenter's notes:** Permeability was measured with effective stress using the AP608 commercial permeameter-porosimeter. Permeability was recorded with incremental increase of effective pressure from 800 to 6000 psi. Since the permeability of the shale matrix is so low, it can be assumed that the measured permeability represents that of the fracture. As pressure increases, the fracture aperture is closed, and permeability decreases.

# Proppants:

Ottawa sand

40/70 mesh

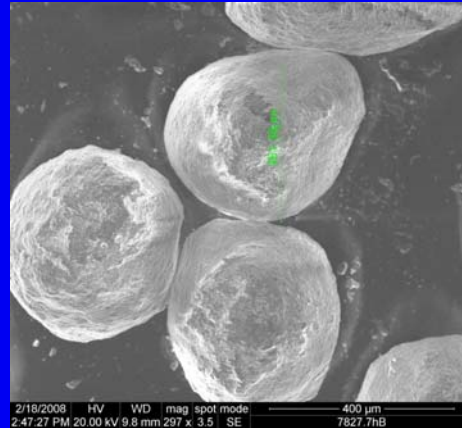
weak



ceramic

40/70 mesh

strong



**Presenter's notes:** Two types of proppant of the same size were used in the proppant experiments, sand and ceramic. Sand is notably weaker than ceramic proppant. Ceramic proppant, though similar in roundness to sand, is much more spherical, and, thus, is expected to be stronger in the face of effective pressure. Convention states that stronger ceramic proppant should perform better in a hydraulic fracturing process, but our research suggests otherwise, leading us to a somewhat novel approach to fracture design.

# Proppant Distribution (sand and ceramic)

Monolayer



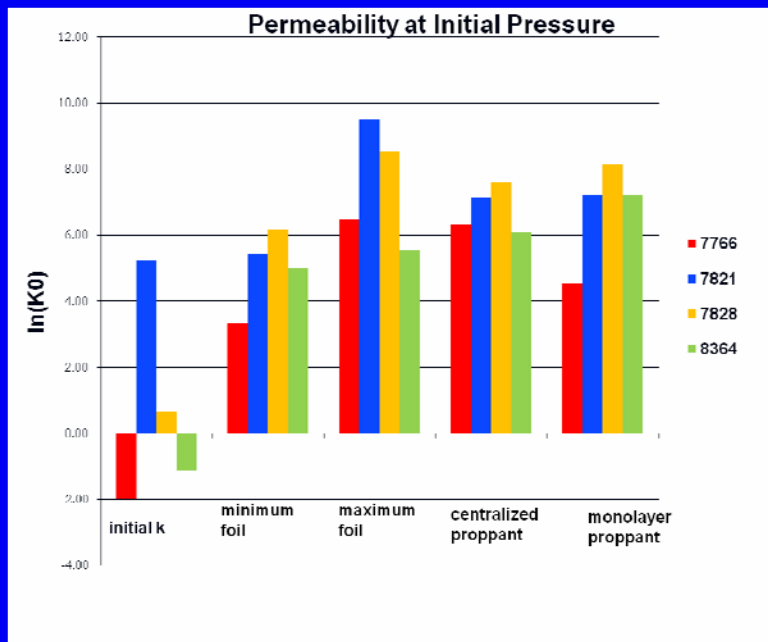
Centralized



More accurately represents proppant distribution in a hydraulic fracture

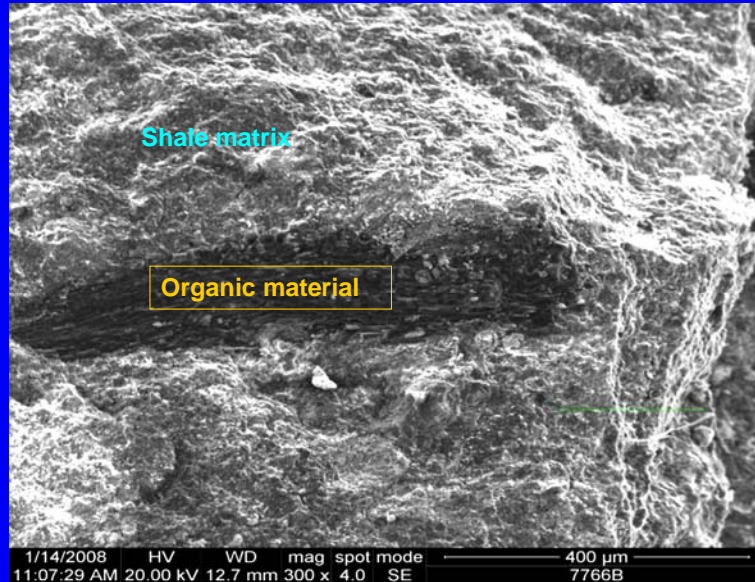
**Presenter's notes:** Permeability of the samples was measured with both types of proppant in two different configurations. The first is a monolayer, evenly covering the entire sample. The second is a central fairway, which more accurately represents proppant distribution in-situ.

## Permeability at $P_0$



**Presenter's notes:** Permeability measurements at initial pressure (~800 psi) for each experiment show that increasing fracture face offset and the use of proppant lead to higher permeability. The more fracture face offset, the higher the permeability. Interestingly, the highest permeability measurements occurred in the sample in which the two fracture faces were the most misaligned, with comparable, and even higher permeability than the samples with proppant.

# SEM Imaging



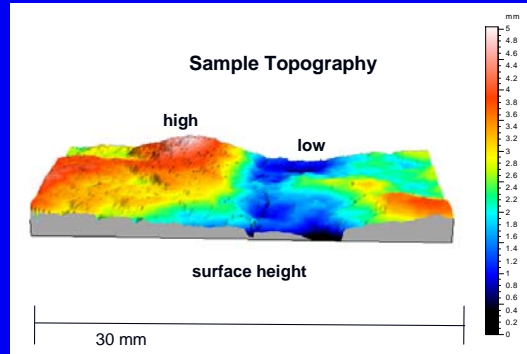
7766

Initial fracture surface with organic inclusion

**Presenter's notes:** A scanning electron microscope image of an original sample surface shows the shale matrix in light gray with an organic inclusion in the dark gray. This typically represents the original fracture surfaces. The surfaces were monitored using the SEM throughout the series of experiments.

# Roughness Profiling

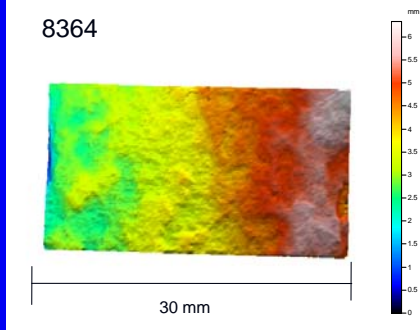
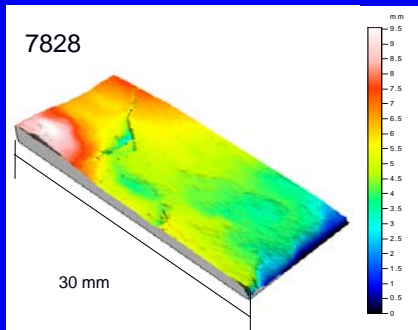
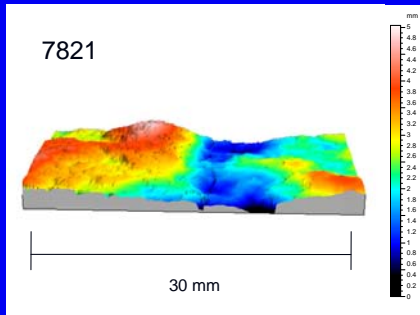
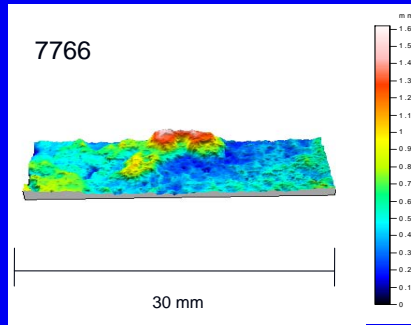
- Roughness characterized using a profilometer
- 3 Parameters, Brown (1987)
  - Fractal Dimension
  - rms asperity height
  - Length scale



Sample 7821A

**Presenter's notes:** Roughness of the samples was characterized using a laser profilometer. In the figure, a topographic representation of a fracture surface, red represents high and blue represents low. According to Brown (1987), three parameters are important in characterizing roughness. Fractal dimension (D) is a statistical quantity that gives an indication of how completely a fractal appears to fill space, as one zooms down to finer and finer scales. Root mean square asperity height is a mathematical representation of the highs and lows present on the fracture face. Also important is the length scale upon which these two parameters were taken.

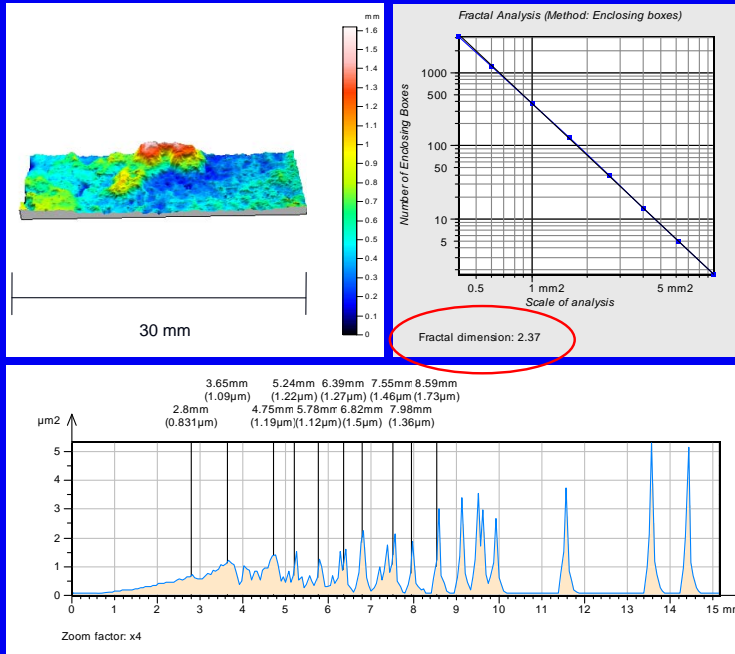
# Roughness Profiling



**Presenter's notes:** The topographic roughness profiles of a representative face from each sample are shown here. Each sample has a unique roughness profile, generated upon fracturing according to the stress properties of the rock. Some samples are much smoother than others. It is important to note the correlation of roughness profiles to permeability.

# Results: Roughness Characterization- Sample 7766 A

rms  
asperity  
height =  
0.223



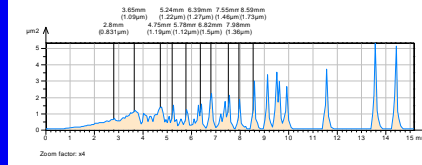
**Presenter's notes:** The laser profilometer generates statistical analyses of the roughness of samples. The spectral analysis of the asperity heights shows amplitude (area in  $\mu\text{m}^2$ ) on the y-axis, and wavelength (height in mm) on the x-axis. This represents an areal weighting of each size feature, showing, most prominently, those that dominate the sample face.

Fractal dimension (upper right) on the sample length scale, is, theoretically, a number that lies between 1 and 3 (1 representing a line, 2 representing a plane, and 3 representing a volume). These samples should lie between 2 and 3. The higher the fractal dimension value, the rougher the sample, and presumably, the higher permeability created by fracture misregistration.

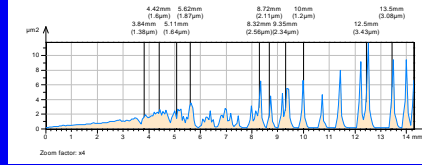


# Spectral Characteristics

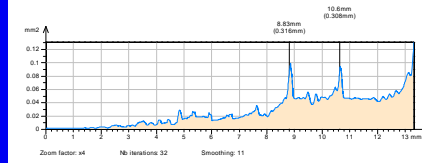
7766



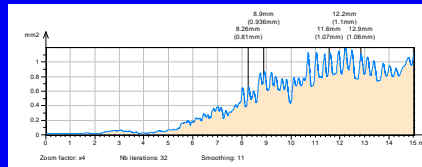
7821



7828.7



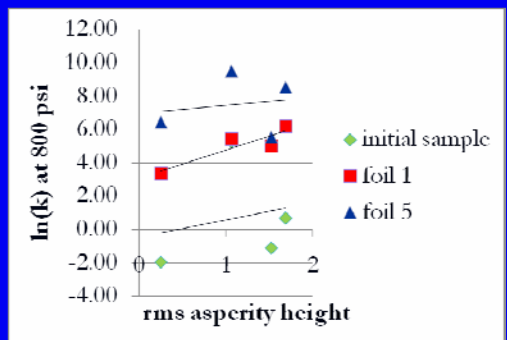
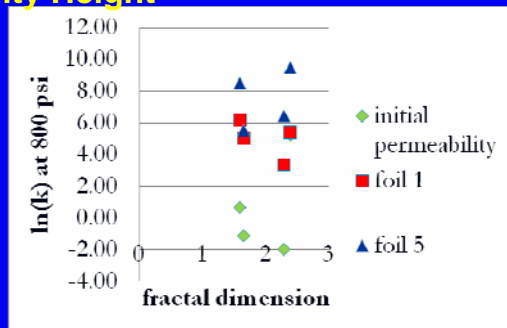
8364



rms height	fractal dimension
0.2525	2.295
1.0655	2.395
1.69	1.6
1.5255	1.66

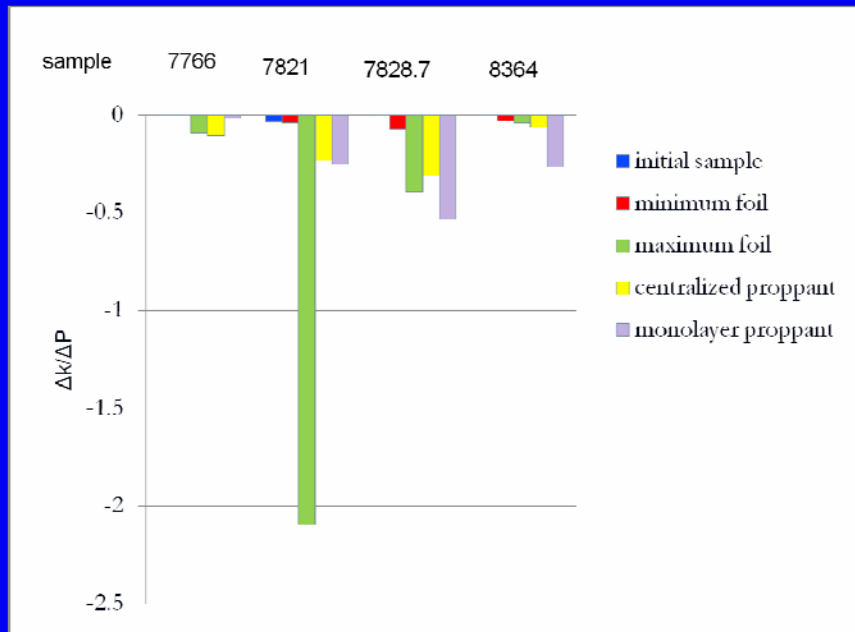
**Presenter's notes:** A comparison of spectral characteristics for each sample clearly shows a broad grouping of “rough” and “smooth” samples. The upper two spectral analyses show the rougher samples with higher peaks and more separation between characteristics. This is also represented in the higher fractal dimension values.

## Initial Permeability Variance with Fractal Dimension and rms Asperity Height



**Presenter's notes:** Initial permeability variance with fractal dimension does not show much of a trend, probably because fractal dimension range is very small, and the data points are limited. The trend of root mean square asperity height against initial permeability is clearer. The plot shows that the rougher the sample, the higher the permeability will be.

## Permeability Variation with Pressure



**Presenter's notes:** Change in permeability with pressure for each experiment and each sample shows that as pressure increases, the fracture aperture closes and permeability decreases (hence negative values). The highest permeability variance with pressure occurred with the maximum fracture face offset.

# Pressure -Dependent Fracture Permeability: Theory

- Walsh model (1981): aperture and tortuosity effects

$$\left( \frac{k}{k_o} \right)^{1/3} = 1 - \left( \frac{\sqrt{2}h}{a_o} \right) \ln \left( \frac{P}{P_o} \right)$$

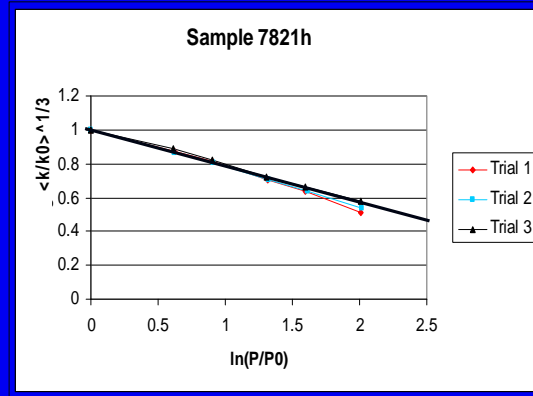
Plot of  $(k/k_o)^{1/3}$  vs  $\ln(P/P_o)$  should be linear

- At  $P_o = 800$  psi
- $k_o$  is permeability
- $a_o$  is aperture
- $h$  is roughness

**Presenter's notes:** H= rms asperity height. According to Walsh, a plot of the cubed root of normalized permeability versus the natural log of normalized pressure should be linear. Assuming initial aperture is constant, any deviation from linearity would be due to a change in roughness (h).

## Results: Pressure Dependence Initial Samples

- Permeabilities effectively followed the theoretical model
- Permeability decreases with increasing effective pressure due to
  - Aperture decrease
  - Tortuosity increase

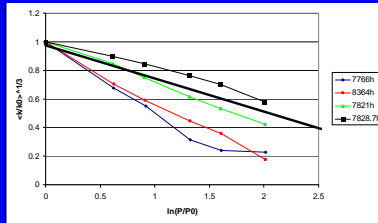


Initial Sample

**Presenter's notes:** The Walsh plot  $(k/k_0)^{1/3}$  vs.  $\ln(k/k_0)$  for the virgin samples appears linear, as expected. Permeability decreases with increasing effective pressure because of the closing of the aperture and an increase in tortuosity, or the convoluted path through which fluid must flow. Additionally, no hysteresis is observable between three trials.

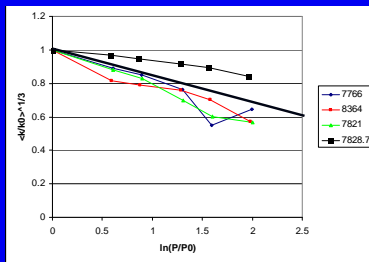
# Results: Offset Faces

Minimum Offset = 0.004"



- Offset data did not follow theory
- Permeability increase is proportional to magnitude of offset
- Asperities out of registration increase aperture and permeability (change in  $h$ )

Maximum Offset = 0.020"



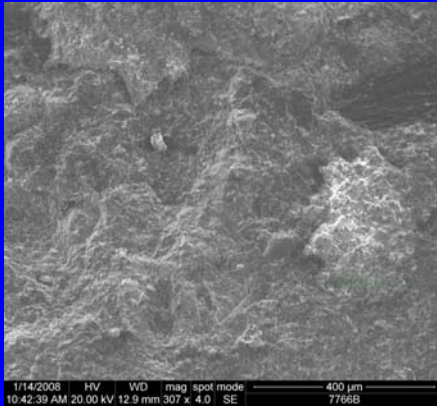
**Presenter's notes:** The Walsh plot for the fracture face offset experiments appears non-linear, though permeability increase is proportional to the magnitude of the offset. As the asperities move out of registration and aperture increases, permeability increases and roughness changes. The change in roughness causes deviation from Walsh's theory.

Non-linear,  $\text{perm} = f(\text{offset})$  on histogram.

Pressure dependence is change in perchange in pressure.

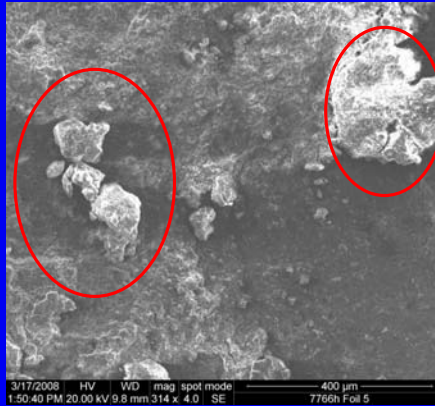
# Surface damage noted after experiment

Original surface



7766h

After pressure measurements  
with offset faces



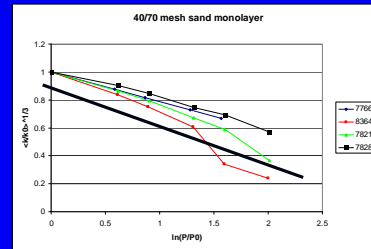
7766h offset = 0.020"

**Presenter's notes:** Scanning Electron Microscope images display the change in roughness (h) after foil offset experiments. The offset of fracture faces causes asperities to move out of registration, and the application of effective confining pressure leads to the crushing of those asperities and changes in the sample surface. This change in h, as previously discussed, causes a deviation from linearity in Walsh's model.

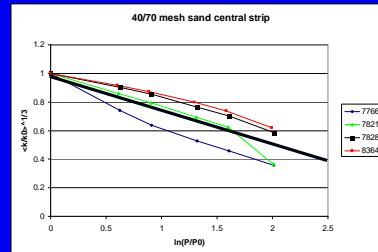
# Results: Proppant Distribution

- Permeability,  $k$ , increase by x 1000
- Almost linear behavior until proppant embedment or fracture
- $k_{\text{central sand}} > k_{\text{mono sand}}$
- $k_{\text{mono ceramic}} > k_{\text{central ceramic}}$
- Proppant perm  $\cong$  greatest offset perm

## Sand Monolayer



## Sand Centralized Strip

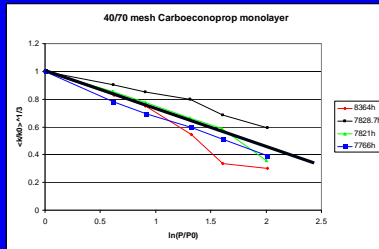


**Presenter's notes:** The monolayer configuration of 40/70 mesh Ottawa sand yielded permeabilities which showed more dispersion between samples than the fairway layer at high pressures. Permeabilities behaved linearly according to the Walsh model until a pressure at which, presumably, proppant starting breaking. The differences between monolayer and centralized sand configurations were about 200 md, within the same order of magnitude. Monolayer is comparable to centralized layer, indicating that if proppant can be evenly dispersed within a fracture, less would be necessary to get the same effect. This has serious economic implications in industry application.



# Results: (Proppant) Sand vs Ceramic

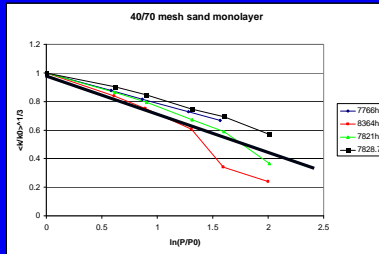
## Ceramic Monolayer



- Obeys simple model until proppant embedment or fracture

- $k_{\text{sand}} > k_{\text{ceramic}}$

## Sand Monolayer

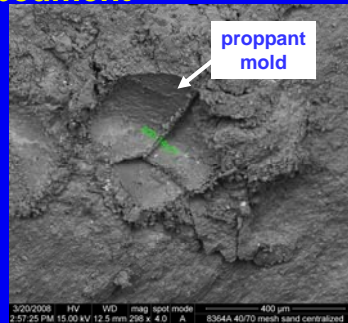


- Embedment of both proppants

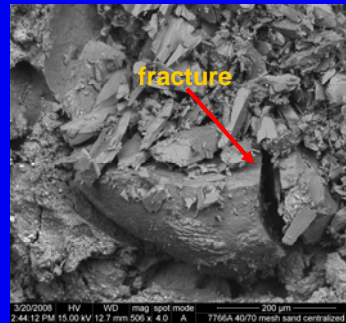
- Sand grain failure causes microcracks

**Presenter's notes:** Both sand and ceramic proppant seem to obey the simple Walsh model until the point at which breaks under pressure or embeds in the shale matrix. At this point, there occurs a deviation from linearity. Overall, higher permeability was seen in the experiments with sand than in those with ceramic (stronger) proppant. Notably, both proppants embedded into the shale matrix, but only the weaker sand failed under pressure. This sudden failure with pressure caused the sand grains to quickly release energy, create microcracks that contributed significantly to the permeability.

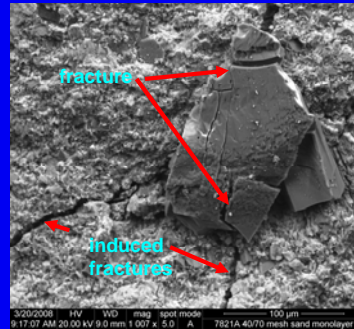
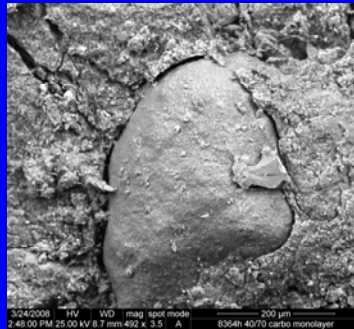
# Embedment



Ceramic



Sand



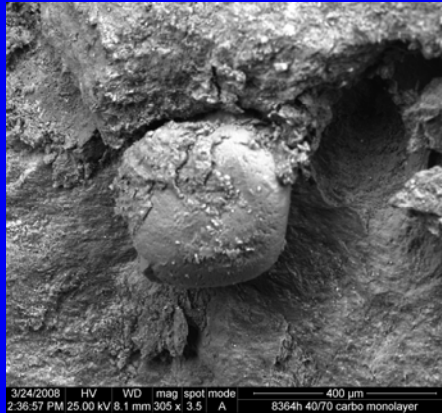
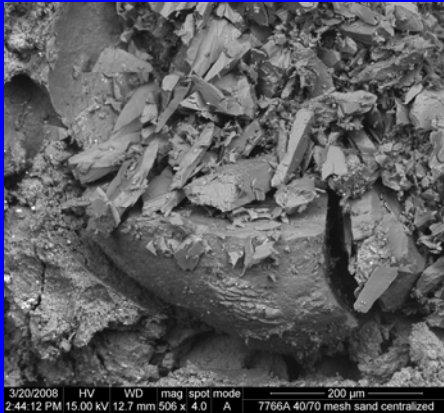
Note: magnifications not equal

**Presenter's notes:** Scanning Electron Microscope images show ceramic proppant (left) embedded in the matrix but not fractured. The sand grains (right) are both embedded and broken. The bottom right image shows how the failure of the sand grain induced small fractures in the matrix. We believe this is why higher permeability was seen with the use of the weaker proppant, sand. This leads us to a novel shale well completions approach in which using the cheaper, weaker sand as proppant is beneficial.

# Conclusions

- Fracture permeability is dependent on starting surface roughness, but variation with pressure is unclear
- Pressure dependence of permeability of initially fractured samples obeys theoretical model
- Fracture permeability is directly proportional to fracture offset or misregistration
- Fracture misregistration could be used in place of proppant
- Proppants increase permeability by a factor of 1000
- Misregistration and proppant embedment/failure cause deviations from theory
- Proppant failure induces fractures in the host shale to improve hydraulic fracture efficiencies, so proppant can be designed to fail at a desired pressure range

## Questions?



Special thanks to Devon and Apache for sponsoring  
research in the University of Oklahoma's IC<sup>3</sup>  
Laboratory.

# References

- Bernabe, Y., 1986, The effective pressure law for permeability in Chelmsford Granite and Barre Granite, Int. J. Rock Mech. and Min. Sci., 23, 3, 267-275.
- Brown, S. E., 1987, Fluid flow through rock joints: the effect of surface roughness, J. Geophys. Res., 92, 2, 1337-1347.
- Cook, N.G.W., 1992. Natural Joints in Rock- Mechanical, Hydraulic and Seismic Behavior and Properties under Normal Stress. International Journal of Rock Mechanics and Mining Sciences & Geomechanics Abstracts, v. 29, pp. 198-223.
- Coulter, Gerald R., Benton, Edward G., Thompson, Clifford L. "Water Fracs and Sand Quantity: A Barnett Shale Example." SPE 90891, presented at SPE 2004 Annual Technical Conference in Houston, TX, 26- 29 Sep 2004.
- Gangi, A F, 1978. Variation of Whole and Fractured Porous Rock Permeability with Confining Pressure. International Journal of Rock Mechanics and Mining Sciences & Geomechanics Abstracts, vol. 15 no. 5, pp.249-257, Oct 1978.
- Kranz, R. L., A. D. Frankel, T. Engler and C. H. Scholz, 1979, The permeability of whole and jointed Barre Granite, Int. J. Rock Mech. and Min. Sci., 16, 225-234.
- Martineau, D.F., 2007. History of the Newark East Field and the Barnett Shale as a Gas Reservoir. American Association of Petroleum Geologists Bulletin, v. 91, no. 4 , pp. 399–403, Apr, 2007.
- Oilfield Glossary: Hydraulic Fractures. Schlumberger, [www.glossary.oilfield.slb.com/](http://www.glossary.oilfield.slb.com/) Downloaded 21 March 2007.
- Renshaw, C. E., 1995, On the relationship between mechanical and hydraulic apertures in rough-walled fractures, J. Geophys. Res, 100, 12, 24629-24636.
- Walsh, J.B., 1981. Effect of Pore Pressure and Confining Pressure on Fracture Permeability. International Journal of Rock Mechanics and Mining Sciences, vol.18, pp. 429-435, 1981.